EEET ECOLOGICAL ENGINEERING & ENVIRONMENTAL TECHNOLOGY

Ecological Engineering & Environmental Technology 2023, 24(9), 291–299
https://doi.org/10.12912/27197050/174034
ISSN 2719-7050, License CC-BY 4.0

Received: 2023.08.02
Accepted: 2023.10.11
Published: 2023.11.15

Environmental Alpha Radiation from the Soil at a Prehispanic Ancient Sacred Site in Lima, Perú

Félix Díaz[1*], Rafael Liza[2,3], Jhonny Rojas[2], Patrizia Pereyra[2], Maria Elena Lopez[2], Daniel Palacios[2], Laszlo Sajo-Bohus[4,5], Santiago Benites[1]

[1] Vicerrectorado de Investigación, Universidad Autónoma del Perú, Panamericana Sur Km. 16,3. Villa El Salvador, Lima 15842, Peru

[2] Departamento de Ciencias, Sección Física, Pontificia Universidad Católica del Perú, Av. Universitaria 1801, San Miguel 15088, Peru

[3] Dirección de Gestión Académica, Universidad Tecnológica del Perú, Av. El Sol 235, Canto Grande 3 Etapa, Lima 15419, Peru

[4] Laboratorio de Física Nuclear, Universidad Simón Bolívar, Caracas 1080, Venezuela

[5] Alba Regia Technical Faculty, Óbuda University, 800 Szekesfehervar, Hungary

* Corresponding author's e-mail: felix.diaz@autonoma.edu.pe

ABSTRACT

In the present work, we investigate the concentration of radon and its alpha-emitting progeny at the archaeological site of *Huaca 20* in Lima, Peru. The site holds significant cultural and historical importance as an ancient pre-Inca ruin, providing valuable insights into the lives and rituals of its former inhabitants. We quantified the radon levels accurately with passive CR-39™ detectors deployed within specially designed chambers at the site for 28 days. In a controlled laboratory environment, we processed the detectors afterward, examining and analyzing the resulting tracks using advanced microscopy and the ImageJ analysis software. The ground-level concentration of radon and its alpha-emitting progeny was determined, revealing elevated levels ranging from 2.4 ± 0.6 to 8.9 ± 0.9 (kBq/m^3). These findings underscore the unique presence of radon at Huaca 20 and highlight the potential impact on microorganisms at ground level. Likewise, these results can contribute to studies on the radiological risks faced by visitors, excavators and archaeologists. Finally, we show the spatial distribution of radon concentrations within the site by creating an iso-concentration map. The iso-concentration map reveals a relation between areas with elevated radon levels and the good preservation of funerary contexts.

Keywords: alpha particles, Radon, natural radioactivity.

INTRODUCTION

The sacred and ritual archaeological sites that hold cultural and religious significance for the ancient communities of the region in the pre-Columbian cultures of the Andean peoples in South America are called *Huacas*. They can manifest as natural features such as mountains, hills, caves, or water sources considered sacred and venerated due to their connection with deities or spirits in the cosmology of the pre-Columbian cultures. They can also be artificial structures, such as temples or truncated pyramids, built for ceremonial and religious purposes. In Inca culture, *Huacas*, known as *wak'as*, represented interaction between the earthly and spiritual realms. Accordingly, they regarded them as sacred entities, centers of worship, and rituals dedicated to divinities. In the modern context, *Huaca* refers to archaeological remains and ancient sites identified and protected as cultural heritage. These sites provide valuable

insights into religious practices, social organization, and the worldview of ancient Andean civilizations, and they are the subject of study and tourist visits. (Moore 2004; 2016; Decano 2014; Curatola y Szeminski 2016)

Located in the San Miguel district of Lima, Perú, Huaca 20 is an archaeological site within the expansive Maranga Complex, encompassing a vast array of pre-Inca ruins. Occupied from the Early Intermediate Period (100–600 AD) to the Late Intermediate Period (1000–1476 AD), this site distinguishes itself through its remarkably well-preserved architecture and a remarkable assemblage of artifacts. During the 1990s, a team of archaeologists from the Pontificia Universidad Católica del Perú (PUCP) spearheaded the initial excavations at Huaca 20. After unveiling a complex of structures serving residential and ceremonial functions, the site revealed an abundance of burials, offering invaluable insights into the culture and lifestyle of its ancient inhabitants. Among the noteworthy discoveries at *Huaca 20* are an assortment of ceramics, textiles, and jewelry. The ceramics exhibit intricate adornments, featuring geometric patterns interwoven with depictions of animals and plants. Crafted from cotton and wool, the textiles showcase intricate designs and patterns. The jewelry repertoire encompasses beads, pendants, and earrings. The Huaca 20 holds immense significance as an archaeological treasure, providing a profound understanding of pre-Inca civilizations from Perú (Vallenas Chacón et al., 2018). This place has undergone successive occupational phases, encompassing domestic and funerary activities. In the former scenario, the structures predominantly comprised adobe and rounded cobblestone, situated on a clayey and coarse sandy terrain. This terrain underwent substantial modifications due to persistent flooding, primarily attributed to the cyclic manifestation of El Niño phenomena (Ana Cecilia Mauricio 2014; Carlos Olivera Astete, 2014; Fernandini, 2015).

As previously stated, Huaca 20 has undergone multiple investigations. During excavation, workers are subjected to particulate matter exposure and radon gas exhaled from the archeological site's soil. Radon is a naturally occurring radioactive gas that is generated from the decay of uranium and radium within rocks. Radon gas is odorless and colorless, becoming a considerable threat to health, such as the leading cause of lung cancer in non-smokers. (Leenhouts, H.P., 1999). High radon exposures occur in poorly ventilated, enclosed spaces such as mines, basements, bedrooms, and certain workplaces. In this line, archaeological sites under excavation or with poor ventilation, such as temples, tombs, and sanctuaries, are also potential places for high radon exposure (Quarto et al., 2013; Balcázar et al., 2014). High indoor radon concentrations can also play a role in the preservation of human remains and artifacts at certain archaeological sites. The underground site can be considered a low-ventilated room (space or chamber) where the radioactive gas induces local conditions that limit microbial activity. Radon and its progeny release energetic alpha particles that, if absorbed, can damage microbial cells and contribute to preserving organic materials like human remains, wood, leather, and textiles. Microbial activity is reduced by creating a highly ionized matter by Coulomb explosion processes that induce a low rate of microbial decomposition with the outcome that organic materials can be remarkably well-preserved over time. (Lee et al., 2019; Sukanya, Joseph, 2023). From an environmental perspective, releasing radon into the atmosphere can disrupt ecological systems, impacting plant and animal life. Furthermore, some studies assess atmospheric electric field fluctuations arising from variations in conductivity induced by radon exhalation. These observations can indicate some geological processes and be used to monitor aerosols and possible seismic events (Ponomarev et al., 2011). Its diffusion into water sources can affect aquatic ecosystems, presenting potential risks to marine life and the possibility of entering human consumption routes (Viktor et al., 2017; Koppel et al., 2022). Rn^{222} and Rn^{220} (thoron) decay by emitting alpha particles with a half-life of 3.82 days and 55.6 s, respectively. Also, the decay chain of Rn^{222} involves several alpha-emitting progenies. The alpha-emitting progeny in this decay chain include Po^{218}, Po^{214}, and Po^{210}. Similarly, certain alpha-emitting progenies exist in the decay chain of Rn^{220}, such as Po^{216}, Bi^{212}, and Po^{212} (Balakrishnan et al., 2021; Jun et al., 2022). Furthermore, these alpha-emitting progenies possess the affinity to bind with aerosols and dust particles, leading to their subsequent deposition in epithelial cells (Puskin, James, 2006; Mustafa, Krewski, 2009; Nazir et al., 2020). Consequently, the inhalation of radon and its progeny contribute to more than 50% of the natural radiation dose received by humans (Kumari et al., 2015). It is

essential to note that, from now on, when we cite radon and its alpha-emitting progeny, we refer to Rn^{222}, Rn^{220}, and all of their alpha-emitting progeny mentioned above.

Thus, studies have conducted comprehensive analyses to measure radon and its progeny within archaeological sites, notably the Egyptian and Mexican pyramids. These rigorous researches aim to determine the maximum permissible annual doses, considering various occupational variables of workers. Additionally, these efforts have resulted in the implementation of robust guidelines to maintain radon levels within acceptable limits actively, ensuring the preservation and safety of these treasured historical sites (Espinosa et al., 1997; Bigu et al, 2000; Pedro Urra González 2005; El-Kameesy et al., 2016; Salama et al., 2018; Kenawy, Morsy, 2022). This study aims to collect and quantify data on the concentration of radon and its alpha-emitting progeny and calculate their respective doses to develop safety protocols. This assessment is especially relevant for visitors, excavators, and archaeologists, as they are exposed to inhalation of dust particles generated within archaeological sites, which inherently carry radon (and its progeny) and pose the highest radiological hazard.

EXPERIMENTAL PROCEDURE

Huaca 20 has the following coordinates: S 12° 3’ 56.086’’ O 77° 4’ 52.138’’. The study area in *Huaca 20* is characterized by recent fluvial deposits from the Quaternary period affected by periodic flooding due to the rising waters of the Chillon River. These deposits consist of unconsolidated material: fine-grained sands with abundant silt and, to a minor extent, clayey silt. During the measurement period, the average temperature was 29°C, with a humidity range of 85–99%. The concentration measurements of radon and its alpha-emitting progeny were carried out at Huaca 20 using CR-39™ detectors. The places where the detectors were situated are shown in Figure 1. The CR-39™ detectors, composed of polymeric polyallyl diglycol carbonate (PADC), were placed inside specially designed chambers. The chambers were precisely sealed to prevent any external interference or disruptions arising from fluctuations in environmental conditions. The CR-39™ detectors are highly sensitive to alpha particles emitted by radon and its progeny. When alpha particles interact with a solid-state nuclear track detector (SSNTD) CR-39™, they can create latent tracks. These tracks are not visible to the

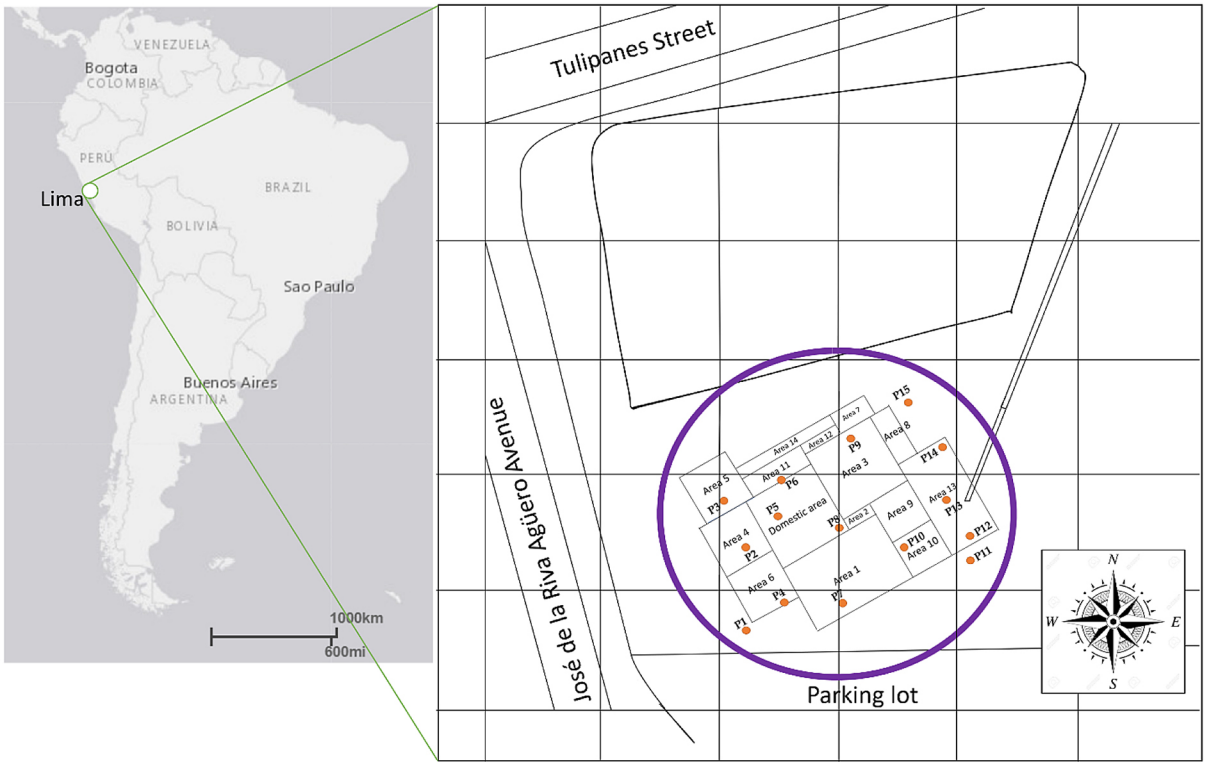

Figure 1. Location map of devices at Huaca 20 archaeological site. The orange points represent the places where the devices were situated

naked eye but can be visible through an optical microscope after a chemical etching process. The etching process removes material from the detector, leaving behind a visible track that records the path of the alpha particle, as shown in Figure 2. By analyzing and counting these tracks, it is possible to estimate the radon concentration and its alpha-emitting progeny from the soil.

We chose the measurement approach (chambers) to minimize potential disruptions in the measurement process and to ensure that the accumulated radon and its progeny were representatives of the site. This methodology allowed for the reliable quantification of radon levels and provided valuable insights into the concentration of radon and its alpha-emitting progeny at *Huaca 20.* Figure 3 presents a detailed schematic illustration of the devices used in the investigation. The devices were positioned at the center of a robust support structure comprising three distinct materials. The support structure, with a surface area ranging from 0.7 m^2 to 1.0 m^2, was designed to ensure reliable and stable placement of the devices. It consisted of an opaque plastic insulator, which effectively prevented any external interference, and a thin aluminum sheet strategically incorporated to increase the impedance for radon escape and to impede the external electromagnetic field that can modify the density track distribution. A total of 15 devices were constructed and subsequently deployed at

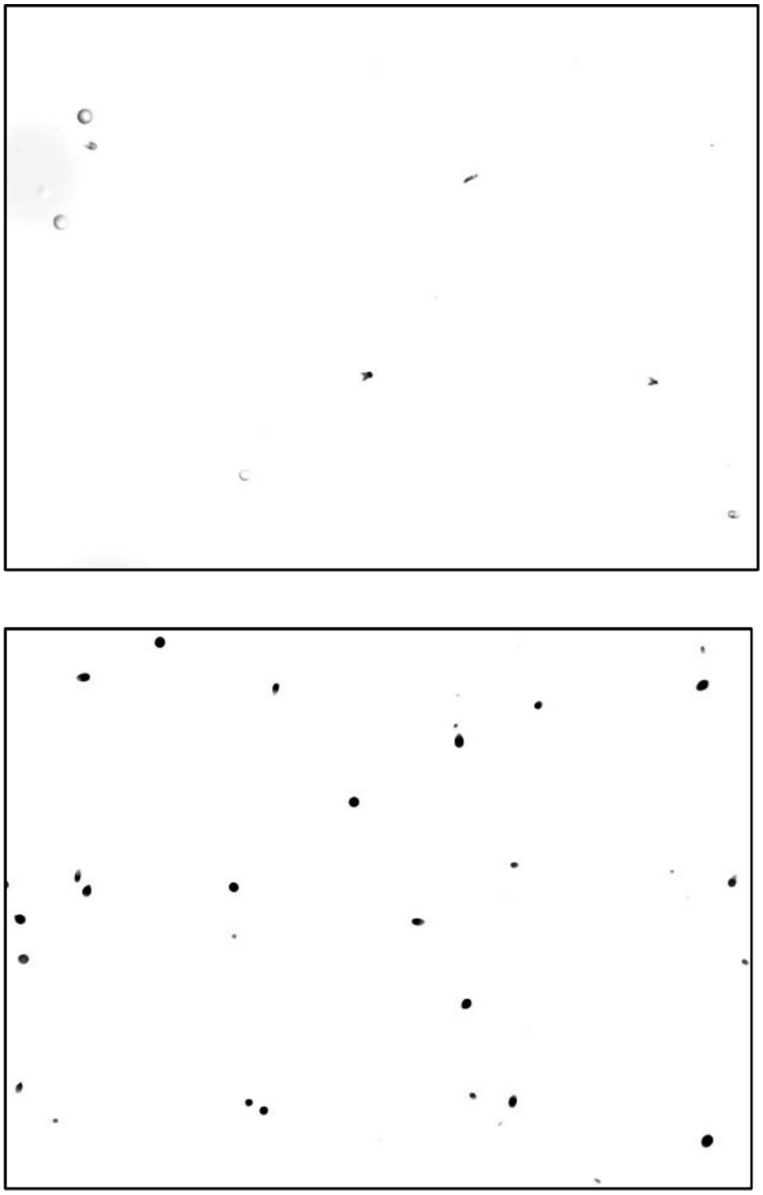

Figure 2. The figure at the top displays a CR-39™ detector without trace signals. The figure at the bottom exhibits a detector after exposure, with alpha tracks particles. These tracks are shown by the rounded black points

ground level for data collection. A secure and consistent setup was established by placing the devices onto the support structure. The edges of the devices measured 20.00 cm in width and were uniformly covered with soil sourced from the excavation site. The soil layer, with a thickness ranging between 5.00 cm and 7.00 cm, served as a protective covering and facilitated the integration of the devices with the surrounding environment. Stones were strategically positioned atop the soil layer to bolster the overall stability and robustness of the system. This additional layer of stones provided structural reinforcement and ensured that the devices remained securely in place throughout the study. By reinforcing the system's rigidity, the stones played a crucial role in maintaining the integrity of the experimental setup.

The placement and construction of the devices, along with the arrangement of the support structure and the incorporation of the soil and stone layers, aimed to establish a reliable and controlled environment for data collection. These measures were essential to minimize any potential sources of interference or bias and to ensure accurate and precise measurements of the targeted variables. We strategically deployed the measurement devices at the archaeological site of *Huaca 20*; their precise geographical placement can be observed in Figure 1. After completing the designated exposure period of 28 days in order to achieve the secular equilibrium between Radon and Radium, we collected the detectors from the site and transported them to the controlled environment of the laboratory for further processing. The subsequent processing involved a designed chemical development procedure. In this procedure, the detectors were subjected to a controlled chemical etching process through immersion in a thermostatic bath containing a 6N NaOH solution. The chemical etching process was conducted at 70°C for 7 hours. The primary objective of this procedure was to trigger a reaction that would unveil the hidden tracks on the detectors.

Subsequently, the revealed tracks on the detectors were examined using LEICA microscopy equipment. A high-powered 20X optical microscope was utilized to visualize the tracks on the detectors, providing enhanced resolution and clarity in their examination. Each detector underwent an analysis, comprehensively examining 35 distinct fields considering an error of less than 10% in the estimation of alpha track density. This comprehensive approach ensured a thorough investigation of the tracks and facilitated the collection of a considerable amount of data for subsequent analysis. We employed *ImageJ* software to facilitate the examination and analysis of the tracks (Bator et al., 2015; Alexandropoulou et al., 2019; Frutos-Puerto et al., 2021). Due to the high density of tracks observed within each field and the need to apply specific visibility criteria such as circularity and track diameter, the software implemented a customized macro. This tailored approach allowed for the efficient and accurate identification, measurement, and analysis of the tracks on the detectors.

RESULTS

The concentration of radon and its alpha-emitting progeny was ascertained by analyzing the obtained readings under the microscope, employing

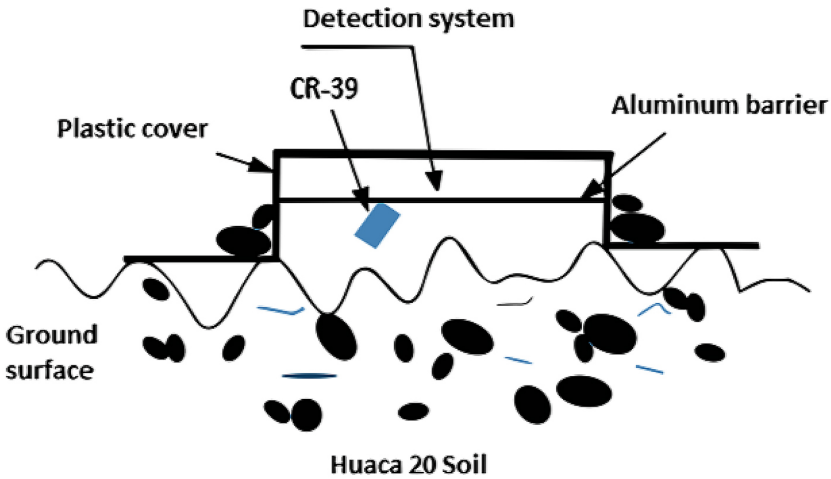

Figure 3. Diagram of the measurement system

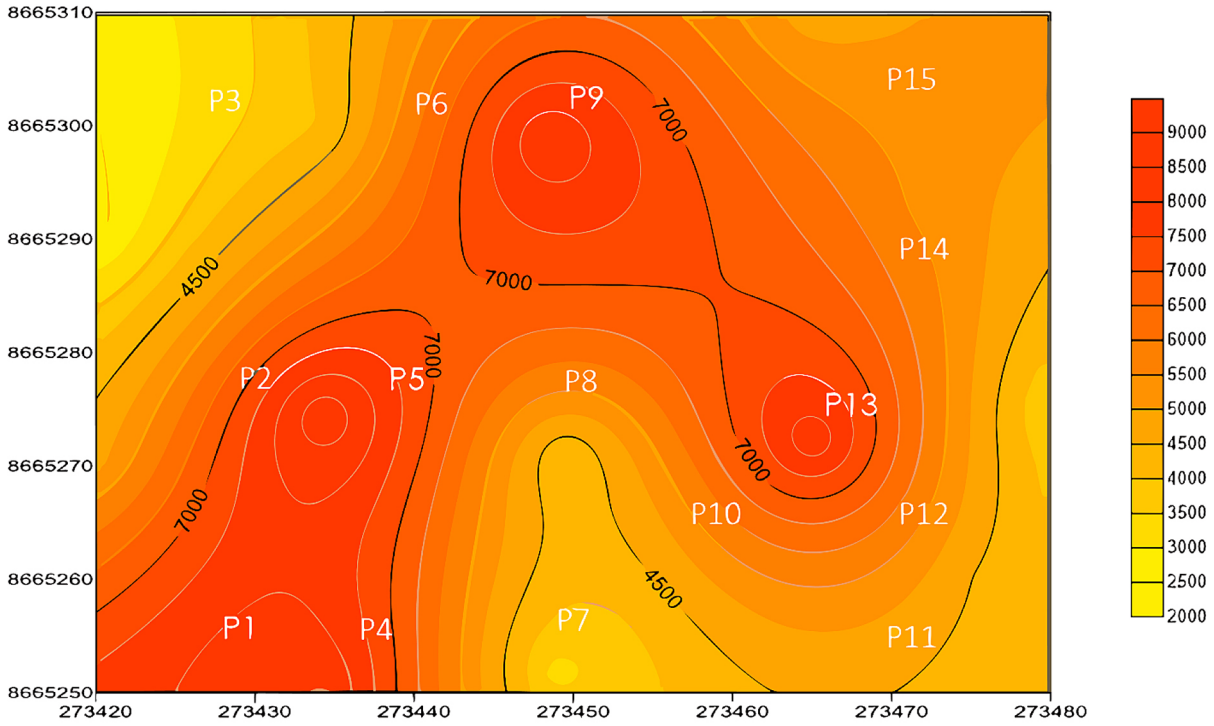

Figure 4. Map of Iso-concentration.

Table 1. Concentration of radon and its alpha-emitting progeny

Detector CR-39™	Concentration *(kBq/m³)*
P1	7.7 ± 1.3
P2	4.9 ± 0.7
P3	2.4 ± 0.6
P4	4.1 ± 0.5
P5	8.9 ± 0.9
P6	8.5 ± 0.8
P7	3.4 ± 0.6
P8	4.0 ± 0.7
P9	8.5 ± 0.8
P10	4.8 ± 1.0
P11	5.3 ± 0.7
P12	5.4 ± 0.8
P13	8.4 ± 0.6
P14	3.5 ± 0.4
P15	4.5 ± 0.4

an appropriate calibration factor as outlined in the study by (Nikolopoulos et al., 2013). Table 1 presents the resulting radon concentration values.

Figure 4 displays the iso-concentration map generated using Surfer 12 software (Golden Software, 2016), providing a visual representation of the spatial distribution of radon concentrations across the Huaca 20. The map serves as a valuable tool for identifying regions with varying levels of radon accumulation. Upon examining the iso-concentration map, it becomes evident that the measurement points exhibiting the best preservation of funerary contexts, as documented by (Fernandini, 2015), align with areas characterized by elevated radon concentrations. These measurement points, labeled explicitly as P1, P5, P9, and P13, emerge as the sites with the highest reported concentration levels of radon and its alpha-emitting progeny.

CONCLUSIONS

The analysis of the concentration levels of radon and its alpha-emitting progeny at the *Huaca 20* archaeological site has revealed compelling findings. The measured values ranged from (2.4 ± 0.6) to (8.9 ± 0.9) (kBq/m³), indicating significantly elevated levels of these radioactive elements. Such concentrations surpass those reported in prior studies focusing on soil (Saad et al., 2013) and building materials (Shoeib, Thabayneh, 2014), drawing attention to the site's uniqueness in terms of radon presence.

Various factors have influenced the *Huaca 20* site throughout history, leading to these remarkable findings. Human interventions and frequent

flooding, predominantly driven by the cyclic appearances of the Niño phenomenon, have played a substantial role in shaping the current radon and alpha-emitting progeny levels. We assume that these factors have created an environment conducive to the accumulation and retention of radon within the site's structures and surrounding soil.

Furthermore, we have observed a relationship between the concentration levels of radon and its alpha-emitting progeny and the preservation of archaeological contexts within the Huaca 20 site. From the findings of the states of the archaeological artifacts reported by (Fernandini, 2015), classified as good, regular, poor, and very poor, and motivated by the findings, we can infer that there is a relationship between the good state of conservation of these artifacts with the areas with the highest concentration of radon according to the iso-concentration map. Although we cannot definitively establish causality at this stage, these findings suggest the importance of further investigations in other Huaca to validate the observed relationship and explore its broader implications.

This study provides compelling evidence of radon and its alpha-emitting progeny concentration levels at the Huaca 20 archaeological site. The unique combination of historical interventions and cyclic flooding events has contributed to this distinctive radon profile. Furthermore, the correlation between radon concentrations and the preservation of archaeological contexts highlights the potential significance of radon as a contributing factor to the site's archaeological integrity because the subsoil environment can act as a natural preservative by inhibiting the growth and activity of microorganisms that would otherwise degrade organic materials. However, it is important to note that the preservation potential of radon depends on various factors, including the geology of the site, the presence of radon-emitting minerals, and the burial conditions of the remains or artifacts. These findings warrant further research and encourage similar studies in other archaeological sites to comprehensively understand the complex interplay between radon, preservation, and the broader archaeological landscape. Additionally, archaeologists and conservationists will find aspects of safeguarding the health of researchers and visitors in this study.

Acknowledgements

This study was carried out as part of the project CAP 2018-3-0018/ PI 578 and the National Council of Science, Technology and Technological Innovation (CONCYTEC) under the Ph.D. scholarship program (236-2015-FONDECYT). The authors thank the GITHUNU-PUCP team.

REFERENCES

1. Alexandropoulou, M., D. Sarigiannidis, C. Papachristodoulou, Stamoulis, K., Ioannides, K.G. 2019. Validation of the ImageJ package for alpha track counting on Solid State Nuclear Track Detectors. HNPS Advances in Nuclear Physics, [online] 24, pp.239–239. doi: https://doi.org/10.12681/hnps.1873.
2. Ana Cecilia Mauricio 2014. Ecodinámicas humanas en Huaca 20: reevaluando el impacto de El Niño a finales del Periodo Intermedio Temprano. Boletín de arqueología PUCP, [online] (18), pp.159–190. doi: https://doi.org/10.18800/boletindearqueologiapucp.201401.008.
3. Balakrishnan, D., Jojo, P.J., Mayeen Uddin Khandaker 2021. Inhalation dose in the indoor environment of Eloor industrial area, Kerala, India. Radiation Physics and Chemistry, [online] 188, pp.109655–109655. doi: https://doi.org/10.1016/j.radphyschem.2021.109655.
4. Balcázar M., Gomez, S.A., P. Peña, J. Zavala Arredondo, Gazzola, J. and A. Villamares (2014). Presence of a radioactive gas in archaeological excavations, determination and mitigation. Applied Radiation and Isotopes. [online] doi: https://doi.org/10.1016/j.apradiso.2013.07.019.
5. Bator, G., Csordás, A., Dávid Horváth, J. Somlai, Tibor Kovács 2015. A comparison of a track shape analysis-based automated slide scanner system with traditional methods. Journal of Radioanalytical and Nuclear Chemistry, [online] 306(1), pp.333–339. doi: https://doi.org/10.1007/s10967-015-4013-9.
6. Bigu, J., Hussein, M.I., Hussein, A.Z. 2000. Radiation measurements in Egyptian pyramids and tombs — occupational exposure of workers and the public. Journal of Environmental Radioactivity, [online] 47(3), pp.245–252. doi: https://doi.org/10.1016/s0265-931x(99)00043-0.
7. Carolyn Dean. 2014, Colonial Latin American Review. (2014). Reviewing Representation: The Subject-object in Pre-Hispanic and Colonial Inka Visual Culture. [online] Available at: https://www.tandfonline.com/doi/abs/10.1080/10609164.2014.972697 [Accessed 22 Aug. 2023].
8. Carlos Olivera Astete 2014. Huaca 20 en el Complejo Maranga: la ocupación lima a inicios del Horizonte Medio. Boletín de arqueología PUCP, [online] (18), pp.191–209. doi: https://doi.org/10.18800/boletindearqueologiapucp.201401.009.
9. Curatola, M. and Szeminski, J. 2016. El Inca y la

huaca: la religión del poder y el poder de la religión en el mundo andino antiguo. Pucp.edu.pe. [online] doi: urn: isbn:9786123171995.

10. El-Kameesy, S.U., Salama, E., S.A. El-Fiki, Ehab, M. y W. Rühm 2016. Radiological safety assessment inside ancient Egyptian tombs in Saqqara. Isotopes in Environmental and Health Studies, [on line] 52(6), pp.567–576. doi: https://doi.org/10.1080/10256016.2016.1142444.
11. Espinosa, G., Manzanilla, L. and Gammage, R.B. 1997. Radon concentrations in the pyramid of the sun at Teotihuacan. Radiation Measurements. [online] doi: https://doi.org/10.1016/s1350-4487(97)00161-3.
12. Fernandini, F. 2015. Innovaciones estilísticas en la cerámica del sitio Huaca 20 a inicios del Horizonte Medio: la presencia Nieveria, en: A. C. Mauricio, L. Muro y C. Olivera (eds.), Huaca 20: un sitio Lima en el antiguo Complejo Maranga. Fondo editorial de la Pontificia Universidad católica del Perú.
13. Frutos-Puerto, S., M.C. Hurtado-Sánchez, de, J., Eduardo Pinilla Gil and C. Miró 2021. Radon alpha track counting on solid state nuclear track detector by an ImageJ-based software macro. Applied Radiation and Isotopes, [online] 173, pp.109695–109695. doi: https://doi.org/10.1016/j.apradiso.2021.109695.
14. Golden Software, LLC. 2016. Surfer for Windows. Contouring and 3-D Surface Mapping.
15. Jun, H., Wu, Y., Miki Arian Saputra, Song, Y., Yang, G. and Shinji Tokonami 2022. Radiation exposure due to 222Rn, 220Rn and their progenies in three metropolises in China and Japan with different air quality levels. Journal of Environmental Radioactivity, [online] 244-245, pp.106830–106830. doi: https://doi.org/10.1016/j.jenvrad.2022.106830.
16. Kenawy, M.A. and Morsy, A.A. 2022. Radon measurements in the interior of the great pyramid. Nuclear Tracks and Radiation Measurements, [online] 19(1-4), pp.347–349. Available at: https://inis.iaea.org/search/search.aspx?orig_q=RN:23027610 [Accessed 23 Aug. 2023].
17. Koppel, D.J., Kho, F., Hastings, A., Crouch, D., MacIntosh, A., Cresswell, T. and Higgins, S. 2022. Current understanding and research needs for ecological risk assessments of naturally occurring radioactive materials (NORM) in subsea oil and gas pipelines. Journal of Environmental Radioactivity, [online] 241, pp.106774–106774. doi: https://doi.org/10.1016/j.jenvrad.2021.106774.
18. Kumari, R., Kant, K. and Garg, M. 2015. The Effect of Grain Size on Radon Exhalation Rate in Natural-dust and Stone-dust Samples. Physics Procedia, [online] 80, pp.128–130. doi: https://doi.org/10.1016/j.phpro.2015.11.078.
19. Leenhouts, H.P. 1999. Radon-induced lung cancer in smokers and non-smokers: risk implications using a two-mutation carcinogenesis model. Radiation and Environmental Biophysics, [online] 38(1), pp.57–71. doi: https://doi.org/10.1007/s004110050138.
20. Lee, K.-Y., Park, S.-Y. y Kim, C.-G. 2019. Effects of radon on soil microbial community and their growth. Environmental Engineering Research, [on line] 25(1), pp.29–35. doi: https://doi.org/10.4491/eer.2018.329.
21. Moore, J.D. 2004. The Social Basis of Sacred Spaces in the Prehispanic Andes: Ritual Landscapes of the Dead in Chimú and Inka Societies. Journal of Archaeological Method and Theory, [online] 11(1), pp.83–124. doi: https://doi.org/10.1023/b:jarm.0000014348.86882.50.
22. Moore, J.D. 2016. Making a huaca: Memory and praxis in prehispanic far northern Peru - Jerry D. Moore, 2010. [online] Journal of Social Archaeology. Available at: https://journals.sagepub.com/doi/10.1177/1469605310381550 [Accessed 22 Aug. 2023].
23. Mustafa Al-Zoughool and Krewski, D. 2009. Health effects of radon: A review of the literature. International Journal of Radiation Biology, [online] 85(1), pp.57–69. doi: https://doi.org/10.1080/09553000802635054.
24. Nazir, S., Shakeel Simnani, Mishra, R., Sharma, T. and Masood, S. 2020. Simultaneous measurements of radon, thoron and their progeny for inhalation dose assessment in indoors of Srinagar, J&K, India. Journal of Radioanalytical and Nuclear Chemistry, [online] 325(1), pp.315–328. doi: https://doi.org/10.1007/s10967-020-07233-2.
25. Nikolopoulos, D., Kottou, S., Petraki, E., Vogiannis, E., Yannakopoulos, P., 2014. Response of CR-39 Polymer Radon-Sensors via Monte-Carlo Modelling and Measurements. Journal of Physical Chemistry & Biophysics. J Phys Chem Biophys 2014, 4:3. DOI: 10.4172/2161-0398.1000144
26. Pedro Urra González 2005. Indoor radon and thoron concentrations in the pyramides of Teotihuacan. Journal of Radioanalytical and Nuclear Chemistry, [online] 264(2), pp.511–516. doi: https://doi.org/10.1007/s10967-005-0746-1.
27. Ponomarev, E.A., Cherneva, N.V. and Firstov, P.P. 2011. Formation of a local atmospheric electric field. Geomagnetism and Aeronomy, [online] 51(3), pp.402–408. doi: https://doi.org/10.1134/s0016793211030145.
28. Puskin, J.S. and James, A. 2006. Radon Exposure Assessment and Dosimetry Applied to Epidemiology and Risk Estimation. Radiation Research, [online] 166(1), pp.193–208. doi: https://doi.org/10.1667/rr3308.1.
29. Quarto, M., Pugliese, M., Loffredo, F., C. Zambella and Roca, V. 2013. Radon measurements and effective dose from radon inhalation estimation in the Neapolitan catacombs. Radiation Protection

Dosimetry, [online] 158(4), pp.442–446. doi: https://doi.org/10.1093/rpd/nct255.

30. Salama, E., Ehab, M. and W. Rühm 2018. Radon and thoron concentrations inside ancient Egyptian tombs at Saqqara region: Time-resolved and seasonal variation measurements. Nuclear Engineering and Technology. [online] doi: https://doi.org/10.1016/j.net.2018.03.017.
31. Saad, A.F., Abdallah, R.M. and Hussein, N.A. 2013. Radon exhalation from Libyan soil samples measured with the SSNTD technique. Applied Radiation and Isotopes, [online] 72, pp.163–168. doi: https://doi.org/10.1016/j.apradiso.2012.11.006.
32. Sukanya S and Joseph, S. 2023. Radon—Mitigatory and Control Measures. Environmental science and engineering, [online] pp.167–184. doi: https://doi.org/10.1007/978-981-99-2672-5_8.
33. Shoeib M.Y. and Thabayneh K.M. 2014. Assessment of natural radiation exposure and radon exhalation rate in various samples of Egyptian building materials. Journal of Radiation Research and Applied Sciences, [online] 7(2), pp.174–181. doi: https://doi.org/10.1016/j.jrras.2014.01.004.
34. Vallenas Chacón, Alain and Heredia, B. 2018. Los Tesoros Culturales de la PUCP: Colección Huaca 20. Pucp.edu.pe. [online] doi: http://repositorio.pucp.edu.pe/index/handle/123456789/112630.
35. Viktor Jobbágy, T. Altzitzoglou, Malo Petya, Tanner, V. and Hult, M. 2017. A brief overview on radon measurements in drinking water. Journal of Environmental Radioactivity, [online] 173, pp.18–24. doi: https://doi.org/10.1016/j.jenvrad.2016.09.019.